Bloch Oscillations of Atoms in an Optical Potential

Maxime Ben Dahan, Ekkehard Peik, Jakob Reichel, Yvan Castin, and Christophe Salomon
Laboratoire Kastler Brossel, Departement de Physique, Ecole Normale Supérieure, 24 rue Lhomond, 75231 Paris Cedex 05, France
(Received 19 January 1996)

Ultracold cesium atoms are prepared in the ground energy band of the potential induced by an optical standing wave. We observe Bloch oscillations of the atoms driven by a constant inertial force. We measure the momentum distribution of Bloch states and effective masses different from the mass of the free atom. [S0031-9007(96)00366-3]

PACS numbers: 32.80.Pj, 03.75.–b

The early quantum theory of electrical conductivity in crystal lattices by Bloch and Zener [1,2] led to the striking prediction that a homogeneous static electric field induces an oscillatory rather than uniform motion of the electrons. These so-called Bloch oscillations have never been observed in natural crystals because the scattering time of the electrons by the lattice defects is much shorter than the Bloch period. In semiconductor superlattices the larger spatial period leads to a much shorter Bloch period ($\sim$600 fs) and Bloch oscillations have recently been observed through the emission of THz radiation by the electrons [3]. Here we present Bloch oscillations of atoms in the fundamental energy band of a periodic optical potential. We directly measure the atomic momentum distribution evolving in time under the influence of a constant inertial force for various potential depths. We experimentally observe oscillation periods in the millisecond range as well as positive and negative effective masses.

Bloch oscillations are a pure quantum effect which can be explained in a simple one-dimensional model. The periodicity of the lattice (period d) leads to a band structure (Fig. 1) of the energy spectrum of the particle and the corresponding eigenenergies $E_n(q)$ and eigenstates $|n, q\rangle$ (Bloch states) are labeled by the discrete band index n and the continuous quasimomentum q; $E_n(q)$ and $|n, q\rangle$ are periodic functions of q with period $2\pi/d$ and q is conventionally restricted to the first Brillouin zone $]-\pi/d, \pi/d]$ [4]. Under the influence of a constant external force F, weak enough not to induce interband transitions, a given Bloch state $|n, q(0)\rangle$ evolves (up to a phase factor) into the state $|n, q(t)\rangle$ according to

$$q(t) = q(0) + Ft/\hbar . \tag{1}$$

This evolution is periodic with a period $\tau_B = h/|F|d$ corresponding to the time required for the quasimomentum to scan a full Brillouin zone. The mean velocity in $|n, q(t)\rangle$

$$\langle v\rangle_n(q(t)) = \frac{1}{\hbar}\frac{dE_n(R(q(t))}{dq} \tag{2}$$

is an oscillatory function of time with zero mean. As a consequence, a wave packet prepared with a well-defined quasimomentum in the nth band will also oscillate in position with an amplitude $\Delta_n/2|F|$ where Δ_n is the energy width of the nth band.

In our experiments the periodic potential results from the light shift of the ground state of atoms illuminated by a laser standing wave. The laser is detuned far from any atomic resonance so that spontaneous emission can be neglected. This configuration was first used in the context of atom diffraction [5] leading to the development of atom optics elements, interferometry [6,7], or studies of quantum chaos [8]. In periodic potentials using lasers closer to resonance, spatial ordering has been observed [9]. In this case the concept of a band structure is useful [10], but experimental evidence for it has only been indirect because spontaneous emission spreads the atom distribution over the whole Brillouin zone [11]. Using one-dimensional Raman laser cooling [12,13] we first prepare a gas of free atoms with a momentum spread $\delta p = \hbar k/4$ in the direction of the standing wave, where $\hbar k$ is the photon momentum. The corresponding atomic coherence length $h/\delta p$ extends over several periods $d = \lambda/2 = \pi/k$ of the optical lattice. By adiabatically switching on the light potential this initial momentum distribution is turned into a statistical mixture of Bloch states in the ground energy band with a quasimomentum width $\delta q = \delta p/\hbar$ much smaller than the

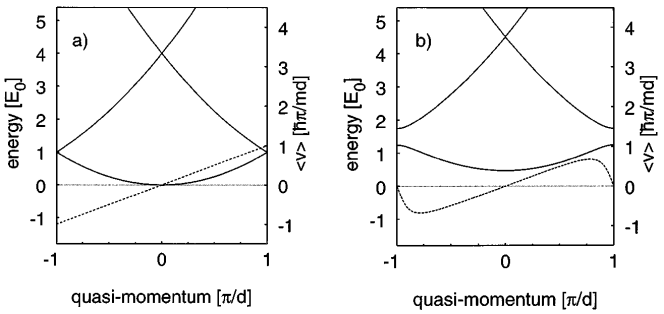

FIG. 1. Band structure $E_n(q)$ (solid line) for a particle in a periodic potential $U(z) = U_0 \sin^2 \pi z/d$ and mean velocity $\langle v\rangle_0(q)$ in the fundamental band (dashed line): (a) free particle case, (b) $U_0 = E_0 = \hbar^2\pi^2/2md^2$. A gap opens at $q = \pm\pi/d$. Under the influence of a weak uniform force, a particle prepared in the fundamental band remains in this band and performs a motion periodic in time called a Bloch oscillation.

 0031-9007/96/76(24)/4508(4)$10.00

width $2k$ of the Brillouin zone. We mimic a constant external force by introducing a tunable frequency difference $\delta\nu(t)$ between the two counterpropagating laser waves creating the optical potential. The reference frame in which the optical potential is stationary is now moving with velocity $\delta\nu(t)\lambda/2$. For a linear variation in time of $\delta\nu(t)$ a constant inertial force $F = -ma = -m\lambda\frac{d}{dt}\delta\nu(t)/2$ is exerted on the atoms in this frame. After a given evolution time t_a, we abruptly switch off the light potential and measure the momentum distribution of the Bloch state at time t_a with a resolution of $\hbar k/18$.

This model system presents several advantages: (i) The initial momentum distribution is well defined and can be tailored at will. (ii) By contrast to solid state systems, the periodic potential, being created by light, can be easily turned on and off. This gives direct access to the momentum distribution of Bloch states. (iii) There is virtually no dissipation or scattering from defects of the potential or from interaction between particles. We observe Bloch periods in the millisecond range, i.e., 10 orders of magnitude longer than in semiconductors.

Our experimental setup for subrecoil laser cooling of cesium atoms has been described previously [13,14]. We use a magneto-optical trap in a low pressure vapor cell to capture atoms and precool them to about 6 μK. After turning off the magnetic field we perform 1D Raman cooling with horizontal beams from two diode lasers that are phase locked to a tunable frequency difference around the cesium hyperfine splitting of 9.12 GHz. We use a sequence of Raman square pulses [13], resonant with velocity classes centered at $\pm v_R$, $\pm 2v_R$, and $\pm 4v_R$ where v_R is the recoil velocity $\hbar k/m = 3.5$ mm/s. In a cooling time of 12 ms this produces a narrow velocity distribution of atoms in the $F = 3$ ground state, with a nearly Lorentzian line shape of half width at half maximum of $0.24v_R$.

After the cooling phase all lasers are switched off except one of the Raman lasers which generates the optical potential. We split it into two beams and pass each of them through an acousto-optic modulator to control its power and frequency. These beams are superimposed onto the horizontal optical axis of the Raman beams in counterpropagating directions. They have the same linear polarization, equal intensities, and are detuned by $\delta/2\pi = 30\,\mathrm{GHz} = 5700\Gamma/2\pi$ from the $6S_{1/2} \rightarrow 6P_{3/2}$ atomic resonance line (wavelength $\lambda = 852$ nm), where $\Gamma/2\pi = 5.3$ MHz is the natural width of the $6P_{3/2}$ state.

Initially the two beams have the same frequency and their dipole coupling to the atom leads to a light shift which is nearly identical for all Zeeman sublevels of $F = 3$ and varies with the atomic position as $U(z) = U_0 \sin^2 kz$. The potential depth is given by $U_0 = (2/3)\hbar\Gamma(I/I_0)(\Gamma/\delta)$, where I is the laser intensity in one beam, $I_0 = 2.2$ mW/cm^2. With a peak intensity of up to 40 mW/cm^2 ($1/\sqrt{e}$ diameter $\approx$4.5 mm) the depth of the potential can be varied between 0 and about $6E_R$ where $E_R = \hbar^2k^2/2m = h \cdot 2.068$ kHz is the recoil energy. Since the spontaneous emission rate is at most 4 s^{-1}, it can be totally neglected during our $\sim$10 ms interaction time.

Initially ($U_0 = 0$) only the Bloch states at the bottom of the ground state energy band are significantly populated. In order to prevent a transfer of population into the higher energy bands the standing wave has to be turned on slowly enough. We have used as adiabaticity criterion the usual condition

$$|\langle n, q|d/dt|0, q\rangle| \ll |E_n(q) - E_0(q)|/\hbar\,. \qquad (3)$$

In the case $U_0 \leq E_R$ the energy difference in (3) for $n = 1$ remains finite [$E_1(0) - E_0(0) \sim 4E_R$] and condition (3) reads $|\frac{d}{dt}U_0/E_R| \ll 32\sqrt{2}E_R/\hbar$ [15]. For larger values of U_0/E_R the energy gap increases and adiabaticity is more easily fulfilled. We use a rise time of 200 μs, largely in the adiabatic regime.

Next a linear frequency ramp of duration t_a up to 8 ms is applied to one of the beams. The resulting inertial force $F = -ma$ has to be small enough to prevent interband transitions which are the most probable when the quasimomentum $q(t)$ given by (1) reaches the edge of the Brillouin zone: For $q = k$ condition (3) imposes $|ma\lambda/2| \ll (\pi/8)U_0^2/E_R$ for $U_0 \leq 10E_R$. We have used accelerations ranging from 0.43 m/s^2 ($d\delta\nu/dt = 10^6$ Hz/s) for a potential depth $U_0 = 0.5E_R$ to 13.2 m/s^2 for $U_0 = 6E_R$. We have checked by a measurement of the final momentum distribution (explained below) that these values do not lead to a significant transfer of atoms to higher bands for several periods of Bloch oscillations. The corresponding frequencies $1/\tau_B$ of the Bloch oscillations are in the range 60 to 1900 Hz.

After a given acceleration time t_a, the standing wave is turned off fast (fall time $\approx$1 μs) so that the free atoms keep the momentum distribution corresponding to the Bloch states. This distribution is probed by a 3 ms long velocity-selective Raman pulse of variable detuning. This pulse transfers atoms in a narrow momentum class (resolution $\hbar k/18$) from the $F = 3$ to the $F = 4$ ground state hyperfine level and the fluorescence signal from these atoms is used to measure their number. Scanning of the Raman detuning gives the atomic momentum distribution in the laboratory frame, from which the distribution in the accelerated frame is obtained by a translation of $-mat_a$.

Figure 2 shows the momentum distribution in the accelerated frame at various times t_a, for $U_0 = 2.3E_R$ and $a = -0.85$ m/s^2. The initial peak shifts linearly with time while its weight decreases. Simultaneously a second peak emerges at a distance $2\hbar k$; its increasing weight becomes equal to the one of the first peak when $t_a = \tau_B/2$ where $\tau_B = 2\hbar k/|F|$. It keeps growing until $t_a = \tau_B$ where the initial momentum distribution is recovered: The atoms have performed a full Bloch oscillation. Further evolution reproduces this pattern periodically.

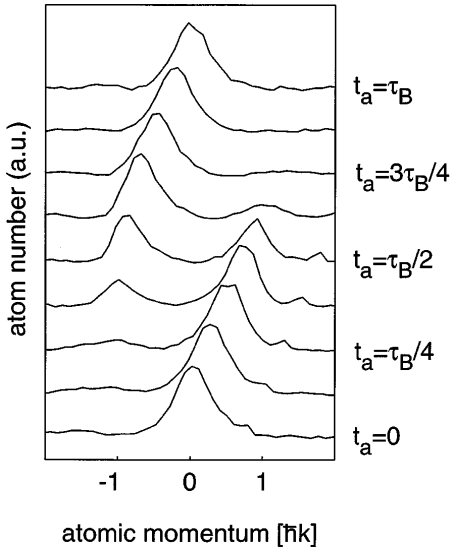

FIG. 2. Bloch oscillations of atoms: momentum distributions in the accelerated frame for equidistant values of the acceleration time t_a between $t_a = 0$ and $t_a = \tau_B = 8.2$ ms. The light potential depth is $U_0 = 2.3E_R$ and the acceleration is $a = -0.85$ m/s^2. The small peak in the right wing of the first five spectra is an artifact.

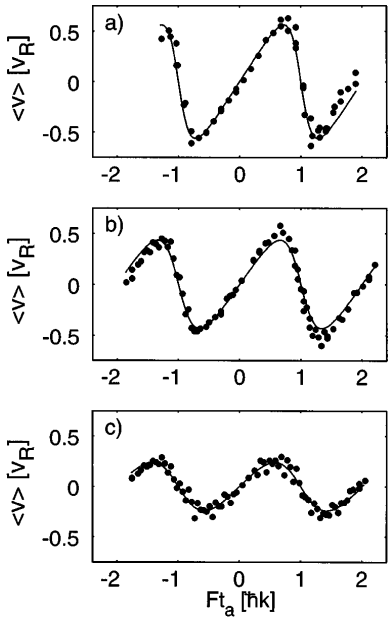

FIG. 3. Mean atomic velocity $\langle v \rangle$ as a function of the acceleration time t_a for three values of the potential depth: (a) $U_0 = 1.4E_R$, (b) $U_0 = 2.3E_R$, (c) $U_0 = 4.4E_R$. The negative values of Ft_a were measured by changing the sign of F. Solid lines: theoretical prediction.

These results can be explained as follows. Bloch states of quasimomentum q are coherent superpositions of plane waves, i.e., momentum states $|p = \hbar(q + 2jk)\rangle$ (j integer). Because of the applied force, q evolves in time according to (1) with the initial condition $q(0) = 0$. In the perturbative case considered here ($U_0 \ll 16E_R$), for $q(t_a) \sim 0$ the Bloch state $|n = 0, q(t_a)\rangle$ is very close to the momentum state $|p = \hbar q(t_a)\rangle$: It has very small populations $[\sim(U_0/16E_R)^2 \simeq 1\%]$ on the $|p = \hbar q(t_a) \pm 2\hbar k\rangle$ momentum states. For $q(t_a)$ close to k, the Bloch state is mainly a linear superposition of the $|p = \hbar q(t_a)\rangle$ and $|p = \hbar[q(t_a) - 2k]\rangle$ momentum states, with equal amplitudes for $q(t_a) = k$, i.e., for $t_a = \tau_B/2$. For $\tau_B/2 < t_a < \tau_B$, $q(t_a)$ scans the $]-k, 0[$ interval of the Brillouin zone and the momentum distribution is turned back into the single initial peak.

In order to further illustrate the oscillatory motion of the atoms, we have deduced from our data the mean atomic velocity as a function of t_a for different values of the potential depth U_0 and for an acceleration $a = \pm 0.85$ m/s^2. We reduce the smoothing effect due to the width of the quasimomentum distribution as follows: We slice the initial momentum peak into narrow channels labeled i, centered at $q_i(0)$ and of width $k/18$. Following the time evolution of each of these slices, we calculate the mean velocity for the atoms in momentum channels $\hbar q_i(t_a), \hbar q_i(t_a) \pm 2\hbar k$ where $q_i(t)$ evolves according to (1). The contributions of the different channels are combined in one curve after a time translation of $\hbar q_i(0)/F$. We have plotted in Fig. 3 the results for three values of U_0/E_R. The measured Bloch periods agree with the expected value (8.2 ms) to within an uncertainty of 4% and do not depend on U_0. For $U_0 = 0.54E_R$ the amplitude of the Bloch oscillations is $0.68\hbar k$ and corresponds to an oscillation in position of 3.1 μm. These amplitudes decrease with growing U_0 [cf. Fig. 4(a)]: The band flattens out as a consequence of the smaller tunnel coupling between neighboring sites of the lattice.

A striking feature of the oscillations presented in Fig. 3 is their asymmetry, which is particularly pronounced for low values of the optical potential: The slope of the mean velocity near the edge of the Brillouin zone ($Ft_a = \pm\hbar k$) is steeper than that near the zone center ($Ft_a = 0, \pm 2\hbar k$). This effect can be described in terms of effective masses: The dynamics of the particle is equivalent to that of a particle in free space: $m^* d\langle v \rangle/dt = F$ with an effective mass $m^*(q)$ given by $\hbar^2/m^* = d^2E_0(q)/dq^2$, which is in general different from the real mass because of the interaction with the potential. In the center and at the edge of the Brillouin zone, the energy band is approximately parabolic, the effective mass is constant, and $\langle v \rangle$ evolves linearly in time. By measuring the slope of $\langle v \rangle(t_a)$ around $t_a = 0$ ($q = 0$) and $t_a = \pm\tau_B/2$ ($q = \pm k$) in Fig. 3, we deduce these two effective masses. In Fig. 4(b), we present their variation with the potential depth U_0. For weak potentials ($U_0 \to 0$), $m^*(q = 0)$ tends to the free atom mass m and $m^*(q = k)$ tends to 0. With increasing potential depth the atoms are more tightly bound and the effective masses increase in absolute value. For

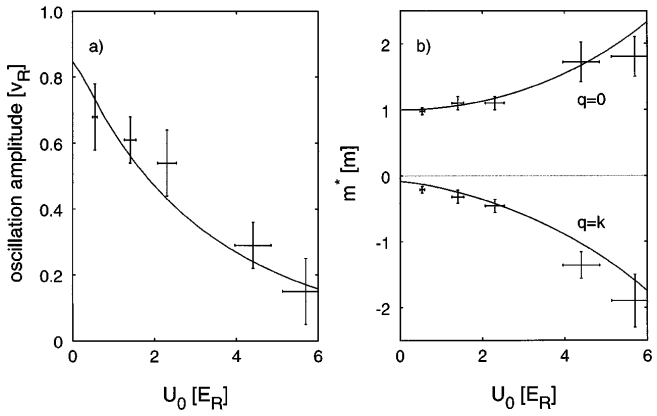

FIG. 4. Amplitude of the Bloch oscillations (a) and effective masses m^* for $q = 0$ and $q = k$ in units of the cesium atomic mass (b) vs potential depth U_0. Solid lines: theory.

$U_0 = 5.7E_R$, $m^*(0)$ is about twice as large as the free mass. In the limit $U_0 \to \infty$ the absolute values of $m^*(0)$ and $m^*(k)$ become equal and diverge as $1/\Delta_0$.

We have calculated numerically the band structure for our experimental values of U_0. The mean velocity of the Bloch states obtained from Eq. (2) is averaged over a statistical mixture of Bloch states corresponding to the experimental resolution, i.e., having a Gaussian distribution of quasimomentum q with standard deviation $k/18$ [16]. The solid lines in Figs. 3 and 4 show the results of these calculations with no adjustable parameter. The agreement with the experimental data is quite good. By integrating over time the data $\langle v(t_a)\rangle$ of Fig. 3 [see Eq. (2)], we have also reconstructed experimentally the fundamental energy band.

Finally we have made preliminary investigations of atom acceleration in the case $U_0 = 5.7E_R$. We could still observe Bloch states after $15\tau_B$. In the laboratory frame, this corresponds to a coherent momentum transfer of $30\hbar k$, producing an atomic beam with subrecoil momentum spread ($\hbar k/4$) in the beam direction. After optimization, this technique should be useful to produce atomic beams with long coherence length from cold atoms prepared in a trap.

We are grateful to C. Cohen-Tannoudji, G. Grynberg, G. Bastard, J. Dalibard, and M. Raizen for stimulating discussions. E. P. and J. R. acknowledge support from the European Union through the HCM program. This work was supported in part by NEDO, CNES, and Collège de France. Laboratoire Kastler Brossel is Unité de Recherche de l'Ecole Normale Supérieure et de l'Université Pierre et Marie Curie, associée au CNRS.

[1] F. Bloch, Z. Phys. **52**, 555 (1929).
[2] C. Zener, Proc. R. Soc. London A **145**, 523 (1934).
[3] C. Waschke, H. Roskos, R. Schwedler, K. Leo, H. Kurz, and K. Köhler, Phys. Rev. Lett. **70**, 3319 (1993).
[4] See, e.g., N. W. Ashcroft and N. D. Mermin, *Solid State Physics* (Saunders, Philadelphia, 1976).
[5] P. L. Gould, G. A. Ruff, and D. E. Pritchard, Phys. Rev. Lett. **56**, 827 (1986); P. J. Martin, B. G. Oldaker, A. H. Miklich, and D. E. Pritchard, Phys. Rev. Lett. **60**, 515 (1988).
[6] For a recent review, see C. S. Adams, M. Sigel, and J. Mlynek, Phys. Rep. **240**, 143 (1994).
[7] E. Rasel, M. Oberthaler, H. Batelaan, J. Schmiedmayer, and A. Zeilinger, Phys. Rev. Lett. **75**, 2633 (1995); D. M. Giltner, R. W. McGowan, and S. A. Lee, Phys. Rev. Lett. **75**, 2638 (1995).
[8] F. L. Moore, J. C. Robinson, C. Bharucha, P. E. Williams, and M. G. Raizen, Phys. Rev. Lett. **73**, 2974 (1994).
[9] For a recent review, see M. G. Prentiss, Science **260**, 1078 (1993).
[10] Y. Castin and J. Dalibard, Europhys. Lett. **14**, 761 (1991).
[11] M. Doery, M. Widmer, J. Bellanca, E. Vredenbregt, T. Bergeman, and H. Metcalf, Phys. Rev. Lett. **72**, 2546 (1994).
[12] M. Kasevich and S. Chu, Phys. Rev. Lett. **69**, 1741 (1992).
[13] J. Reichel, F. Bardou, M. Ben Dahan, E. Peik, S. Rand, C. Salomon, and C. Cohen-Tannoudji, Phys. Rev. Lett. **75**, 4575 (1995).
[14] J. Reichel, O. Morice, G. M. Tino, and C. Salomon, Europhys. Lett. **28**, 477 (1994).
[15] The adiabaticity criterion would have been more stringent for a value of q closer to the boundary k of the Brillouin zone, where the band gap vanishes with U_0.
[16] The averaging has a significant influence only for the smallest values of U_0 and around $q = \pm k$ where $\langle v\rangle$ changes very quickly. It explains why the oscillation amplitude does not converge to v_R in Fig. 4(a) and why the effective mass $m^*(k)$ does not tend to 0 in Fig. 4(b), for $U_0 \to 0$.